Forest Ecology and Management 354 (2015) 43–55

Contents lists available at ScienceDirect

Forest Ecology and Management

journal homepage: www.elsevier.com/locate/foreco

A generalized tree component biomass model derived from principles of variable allometry

David W. MacFarlane

Department of Forestry, Michigan State University, East Lansing, MI 48824, United States

ARTICLE INFO

Article history:
Received 16 April 2015
Received in revised form 11 June 2015
Accepted 14 June 2015
Available online 9 July 2015

Keywords:
Tree biomass
Allometry
Hardwoods
Mass components

ABSTRACT

Accurate estimates of forest biomass stocks are critical for scientists, policymakers and forest managers trying to address an increasing array of demands on forests, to sustain human well-being and a broader diversity of life forms on Earth. Thus, it is important that forest biomass estimates are translatable into both biologically and economically meaningful components. Here, a new variable-form, variable-density tree mass component model is presented. The model decomposes a tree into a system of tree component-specific equations that: (a) reflect variation in scaling relationships between major portions of the tree body that define variation in whole-tree growth form and (b) relate to commercially relevant portions of the tree. When tested using data collected from felled and dissected hardwood trees of different size and species, growing over a range of stand conditions, the variable-form, variable-density models gave superior predictions for all components of tree mass, when compared to standard fixed-form, fixed-density models that predict tree mass components only from stem diameter at breast height (DBH). The results demonstrated why the standard approach of estimating mass components from DBH with a power function is fairly limited, because base-, trunk-, crown- and main stem-DBH relationships are all variable within and between tree species. Species-specific models were generally superior, but a mixed-species model gave equivalent and sometimes better results than equations fitted to each species individually. The results provide a theoretical basis for biologically-meaningful, robust estimation of tree biomass components over a range of species and forest conditions and may offer new flexibility in producing ecologically and economically relevant biomass inventories.

1. Introduction

Accurate estimates of forest biomass stocks are critical for scientists, policymakers and forest managers trying to address an increasing array of demands on forests, to sustain human well-being and a broader diversity of life forms on Earth. With broad concern about global climate change, it is recognized that forests are important global sinks for CO_2 (Domke et al., 2012a; Chave et al., 2014), as well as sources of biologically renewable products and fuels (Domke et al., 2012b). The Food and Agricultural Organization of the United Nations (FAO, 2010) recently estimated that thirty percent of the world's forests are primarily used for production of wood and non-wood forest products. In the USA, forest fluxes (including that from harvested wood) accounted for 88% of total 2012 net CO_2 flux (USEPA, 2014). Therefore, it is important that forest biomass estimates are translatable into both biologically and economically meaningful components.

Since standing trees cannot be weighed, estimates of forest biomass come principally from tree biomass equations, which are applied to measurements of trees during forest inventories. So, improving tree biomass equations is fundamental to improving forest stock estimates (Chave et al., 2014; Sileshi, 2014; Weiskittel et al., 2015). The standard tree mass equation predicts total tree mass as a power function of stem diameter at breast height (DBH):

$$M_W = \alpha D^{\beta} \quad (1)$$

where M_W (kg) is the above-ground dry mass of a tree, D (cm) is its DBH (measured 1.3 m above ground) and α and β are coefficients to be estimated for a population of trees. This equation has biologically meaningful coefficients relating to the theory of "allometric" scaling relationships, which are relationships between the sizes of different parts of an organism relative to the whole (Huxley and Tessier, 1936). For example, a metabolic scaling theory predicts a universal relationship of $M = \alpha D^{8/3}$ (e.g., West et al., 1999; Enquist, 2002). Allometric relationships often take the form of a power equation

E-mail address: macfar24@msu.edu

http://dx.doi.org/10.1016/j.foreco.2015.06.038
0378-1127/

(Stevens, 2009), as in Eq. (1), but need not be confined to any particular mathematical form.

Though biologically interesting, the generality of simple allometric models has been called into question because allometric scaling relationships are apparently non-stationary within species, across the large spatial domains over which tree biomass equations are typically applied (Ducey, 2012). Niklas (1995) demonstrated that allometric relationships change, even within the lifetime of individuals of a single species, growing under homogenized conditions, and cited this "size-dependent" allometry as evidence that no universal allometric scaling coefficients could be estimated for trees. Further, Chave et al. (2009) demonstrated a high degree of variability in relationships between tree size and wood density, reinforcing findings that simple dimensional measurements may be insufficient for accurate estimation of tree mass, in the face of varying wood density (Chave et al., 2005).

Ketterings et al. (2001) showed how Eq. (1) could be generalized to explicitly reference tree height (H) and density (ρ), with the assumption that $H \propto D^{\gamma}$ making β in Eq. (1) equal to $2+\gamma$, and $\alpha \propto \rho$. This work provides a theoretical linkage from Eq. (1) to a more generalized and biologically meaningful "form-factor" model for tree biomass (modified here from Cannell, 1984):

$$M_W = F\rho\frac{\pi}{4}D^2H \tag{2}$$

where H (m) is total tree height above ground, ρ is its density (kg m^{-3}, measured 1.3 m above ground) and F is a 'whole-tree' form factor (Gray, 1966; Cannell, 1984) for indexing the mass of a tree, relative to a proxy mass which is a proxy tree volume $\left(\frac{\pi}{4}D^2H\right)$ multiplied by tree density (i.e., $\rho\frac{\pi}{4}D^2H$).

Eq. (2) has been advocated as a generalized tree biomass model, useful over a range of species and forest ecosystems across the globe (Cannell, 1984; Chave et al., 2014), with an alternative form that allows for non-proportional scaling relationships between M_W and proxy tree mass:

$$M_W = F\left(\rho\frac{\pi}{4}D^2H\right)^B \tag{2a}$$

When $B \neq 1$, the relationship is not proportional, indicating that form changes as the tree changes in mass.

While allometric scaling relationships have been fundamental to understanding the eco-physiology of tree species and forest ecosystems worldwide (Enquist, 2002), they also have economic meaning relevant to forest management. For example, greater allocation of tree biomass to main stem versus branch components has important implications for forest utilization (Adu-Bredu et al., 2008; MacFarlane, 2011), because the most valuable parts of trees are in straight, sound parts of the main stem and the less valuable portions are in branches. While branches are much more likely to be utilized for biomass fuel or remain as slash on the forest floor, they also contain disproportionate fractions of nitrogen and other nutrients critical for sustaining forest productivity (Egnell and Valinger, 2003). Thus, improved estimation of tree biomass components is of value to forests managers as well as tree biologists.

Simple allometric models (like Eq. (1)) have been widely used to predict components of tree biomass (e.g., branches, bole, stump) from DBH (e.g., Bi et al., 2004, Brandeis et al., 2006), but there is substantial evidence that DBH is a generally poor predictor of component fractions of whole-tree biomass (Jenkins et al., 2003; Weiskittel et al., 2015). This likely relates to important differences in the scaling of tree parts, relative to the whole, i.e. allometry. For example, trees with disproportionally large crowns can have different total mass-DBH relationships than those with more proportional crowns (Goodman et al., 2014). This suggests that improved estimation of biomass components could also help improve estimation of whole-tree mass.

Here, a new tree mass component model, derived from Eq. (2), is presented. The model was developed with three major goals in mind: (1) the model should incorporate prevailing scientific theories of tree allometry; (2) total tree biomass would be estimated as the sum of major biologically- and economically-important components of the tree; (3) the model would be robust across multiple species, growing under different forest conditions, based on an underlying hypothesis that species differences could be captured by general relationships describing variability in tree form and wood density. In the sections that follow, the model is described and then tested using data collected from felled and dissected hardwood trees of different size and species, growing over a range of stand conditions. The model is then compared with an alternative model that uses only DBH to predict each major tree mass component and three prevailing models for predicting whole-tree mass (Eqs. (1), (2) and (2a)).

2. A variable-form, variable-density tree mass component model

2.1. Theoretical background for model derivation

Derivation of a new tree mass component model from the form-factor model (Eq. (2)) was based on the idea that different parts of the tree change in shape as trees increase in size and should have allometric scaling coefficients that differ from that of the whole tree (i.e., allometric scaling is not isometric). Most scientific studies of tree form have been focused on the main stem of the tree, producing large numbers of stem profile (a.k.a. "taper") models to describe changes in the shape of the main stem from tree base to top (Kozak, 2004). By contrast, the prevailing theories of allometric scaling in trees are directly or indirectly based on tree branching architecture; these are: (1) pipe model theory, which is based on Da Vinci's model of a constant cross-sectional area of stems as they split into branches (Van Noordwijk and Mulia, 2002), (2) metabolic scaling theory (West et al., 1999), which suggests universal allometric scaling based on fractal-like branching networks, and (3) several variants of models based on mechanical stress principles, where the form of the tree is a response to wind and gravitational loading of the crown on the trunk of the tree (Eloy, 2011). An important paper by Mäkelä and Valentine (2006) united key elements of these theories by highlighting that (a) fractal branching geometry only pertains to the crown of the tree and (b) tapering of the trunk below the crown is a direct reflection of past branching events and branch losses. Recent empirical studies of tree fractal branching by MacFarlane et al. (2014) confirmed that divergence of real trees from theoretical fractal trees was due to variation in the size and tapering of the trunk relative to the crown, along with constraints on crown spread due to constrained growing space. So, both theoretical and empirical studies suggest that separating out the crown and trunk components and recognizing both internal and external constraints on tree crown expansion are critical to explaining more of the variation in tree mass allometry.

2.2. Vertical segmentation of tree form

The currently-accepted paradigm for modeling stem form suggests that the main stem can be divided into three vertical segments: the base, middle and top of the tree, which are approximately neolodial, parabaloidal and conical in shape, respectively (Zakrzewski and MacFarlane, 2006). In reality, stem geometry is more complex than that and a number of studies have

indicated that changes in main stem form are linked to crown size (Muhairwe, 1994; Valentine and Gregoire, 2001; MacFarlane, 2010), suggesting that a crown-segmented model would be appropriate for modeling cumulative tree mass in a tree height profile (Ver Planck and MacFarlane, 2015). Based on this concept, a new, vertically-segmented mass component model was derived from Eq. (2), by dividing a tree into three mass components, M_1, M_2 and M_3, which are, respectively, the mass of the tree from base to DBH, the mass of the trunk above breast height, but below the crown base, and the mass of the crown (Fig. 1):

$$M_1 = F_1\left[\rho\frac{\pi}{4}D^2(H_B)\right] \tag{3a}$$

$$M_2 = F_2\left[\rho\frac{\pi}{4}D^2(H_C - H_B)\right] \tag{3b}$$

$$M_3 = F_3\left[\rho\frac{\pi}{4}D^2(H - H_C)\right] \tag{3c}$$

where H_B is breast height (1.3 m), H_C (m) is the height to the base of the live crown, where the live first branch is attached to the trunk, and coefficients F_1, F_2 and F_3 are unitless form coefficients. Whole-tree mass is given as:

$$M_W = M_1 + M_2 + M_3 \tag{3}$$

Thus, the tree is the sum of its parts, each of which has measurable dimensions and its own form coefficient, instead of having a single form coefficient to describe the shape of the whole tree (as in Eq. (2)).

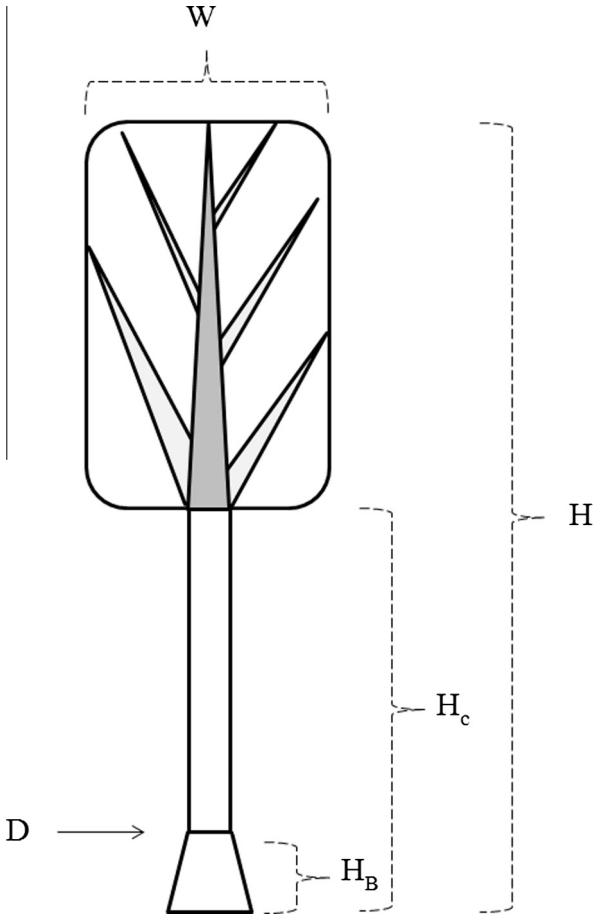

Fig. 1. A basic model of a tree, showing tree mass components and associated dimensional variables: D is stem diameter at breast height, H_B is breast height, H_C is height to base of live crown, H is total height and W is average crown spread. The gray-shaded portion of the main stem is the dominant stem inside the crown.

2.3. Differentiation of the dominant stem in the crown

While Eq. (3) allows for separate parameterization of major components of tree form, further differentiation of the crown was needed to separate the merchantable portion of the main stem from the branches (see MacFarlane, 2010, 2011 and Ver Planck and MacFarlane, 2014). Because the relative allocation of mass to the main stem is so important to the commercial valuation of a tree (Jordan et al., 2006) and because the size of the main stem inside the crown, relative to the size of competing branches, is an indicator of fractal branching architecture (Van Noordwijk and Mulia, 2002), Eq. (3) was further modified to separate out the branches from the 'dominant' stem in the crown (*sensu* Ver Planck and MacFarlane, 2014), which is the continuation of the main stem inside the crown (shaded in Fig. 1). The resultant model is a four-component biomass model:

$$M_W = M_1 + M_2 + M_3 + M_4 \tag{4}$$

with components:

$$M_1 = F_1\left[\rho\frac{\pi}{4}D^2(H_B)\right] \tag{4a}$$

$$M_2 = F_2\left[\rho\frac{\pi}{4}D^2(H_C - H_B)\right] \tag{4b}$$

$$M_3 = F_3\left[\rho\frac{\pi}{4}D^2(H - H_C)\right] \tag{4c}$$

$$M_4 = F_4\left[\rho\frac{\pi}{4}D^2W\right] \tag{4d}$$

where M_3 is now the mass of the dominant stem inside the crown and M_4 is the mass of all (other) branches (Fig. 1), with associated scaling coefficients F_3 and F_4, respectively. M_1 and M_2 are the same as in Eq. (3). W is the average width of the crown (Fig. 1), which captures spreading of the tree in the horizontal, rather than vertical dimension. Note that $\frac{\pi}{4}D^2W$ is an abstract volume with an abstract form coefficient F_4 that indexes the fractal branching architecture of the crown, which, unlike the main stem of the tree, is a complex object that cannot be described using simple Euclidean geometry (Zeide and Pfeifer, 1991). In Eq. (4), whole-tree form varies as a complex function of individual changes in the relative size of the different components.

2.4. Non-proportionality in component form

While Eq. (4) allows for separate parameterization of the relative contribution of major trunk and crown sections to tree mass, it assumes fixed-form scaling for the components themselves, over the attainable size range of the components. This assumption can be relaxed by putting power coefficients (B_i) on predictors of each component of mass to create a 'variable-form, variable-density' mass component model:

$$M_W = \left[F_1\left(\rho\frac{\pi}{4}D^2H_B\right)^{B_1} + F_2\left(\rho\frac{\pi}{4}D^2(H_C - H_B)\right)^{B_2} + F_3\left(\rho\frac{\pi}{4}D^2(H - H_C)\right)^{B_3} + F_4\left(\rho\frac{\pi}{4}D^2W\right)^{B_4}\right] \tag{5}$$

with individual mass components:

$$M_1 = F_1\left[\rho\frac{\pi}{4}D^2(H_B)\right]^{B_1} \tag{5a}$$

$$M_2 = F_2\left[\rho\frac{\pi}{4}D^2H(H_C - H_B)\right]^{B_2} \tag{5b}$$

$$M_3 = F_3\left[\rho\frac{\pi}{4}D^2H(H - H_C)\right]^{B_3} \tag{5c}$$

$$M_4 = F_4\left[\rho\frac{\pi}{4}D^2W\right]^{B_4} \quad (5d)$$

When the value of $B_i \neq 1$, the allometric scaling coefficient (F_i) for a component M_i changes as the component changes in mass. Hence, in Eq. (5), scaling of each tree component is allowed to be size-dependent which, in turn, allows for size-dependent allometric scaling of the whole-tree.

2.5. Fixed-form, fixed-density component mass model

Eq. (5) can be contrasted with a 'fixed-form, fixed-density' mass component model, which assumes a fixed allometric relationship between components and DBH, but not a single power coefficient for whole-tree mass scaling (as in Eq. (1)):

$$M_W = \alpha_1 D^{\beta_1} + \alpha_2 D^{\beta_2} + \alpha_3 D^{\beta_3} + \alpha_4 D^{\beta_4} \quad (6)$$

where α_i and β_i are coefficients to be estimated for a population of trees for the four components of tree mass:

$$M_1 = \alpha_1 D^{\beta_1} \quad (6a)$$

$$M_2 = \alpha_2 D^{\beta_2} \quad (6b)$$

$$M_3 = \alpha_3 D^{\beta_3} \quad (6c)$$

$$M_4 = \alpha_4 D^{\beta_4}. \quad (6d)$$

3. Methods

3.1. Data

Tree data used to test models presented here were collected as part of a broader effort by the Forest Inventory and Analysis (FIA) Program of the United States Department of Agriculture (Bechtold and Patterson, 2005) to develop new national tree biomass equations. FIA provides estimates of changes in the nation's forest biomass and carbon stocks from a national network of forest monitoring plots (Woodall et al., 2011). The FIA program has launched a national-scale effort to obtain regionally-representative data to test exiting models and explore new model forms for estimating total tree mass and tree mass components (Weiskittel et al., 2015), including the ones tested here.

The study region was the southern Lower Peninsula of Michigan (Fig. 2), which has a climate characterized by below-freezing winter temperatures, about 750–900 mm of rainfall per year and a growing season ranging from 140 to 160 days, supporting broad-leaved deciduous (a.k.a. "hardwood") forests (Dickmann, 2004). In different stands, in different forests, individual trees of regionally-important hardwood species were selected to fulfill a matrix of 5 cm DBH classes and canopy classes including suppressed, intermediate, co-dominant, dominant and open-grown trees. The stands included a variety of naturally-regenerated, mixed-species hardwood stands across Lower Michigan. Only live trees without major crown damage were selected for this analysis. Before felling for destructive sampling, each tree selected was measured standing for D, H, and H_C. W was also measured, in two directions at 90° angles from each other, and averaged. Summary statistics for the sample trees and the number of stands each species were drawn from are shown in Table 1.

After standing measurements were completed, trees were cut at a stump height of 15 cm above ground level. Trees were felled into a clearing where debris from other trees had been removed to minimize damage to the crown. The diameter of the main stem was measured at 0.15, 0.8, and 1.3 m above ground and then at 1.2 m intervals following the dominant stem inside the crown to the top. The diameter at H_C was also measured. Trees were cut at 0.15, 1.2, 2.4 m above ground, and then at 1.2 m or 2.4 m intervals along the entire main stem, depending on the size of the tree. The green mass of each main stem section was determined by weighing it on a tractor-mounted crane scale, or an electronic balance for smaller pieces. Disks, approximately 5 cm thick, were cut at 0.15 and 1.3 m and from the top of each cut section. The green mass of each disk, with attached bark, was measured in the field and the dimensions of each disk were measured in multiple directions for computing disk volume.

The basal diameter of every branch on every tree was measured outside the bark, just above the branch collar. For branches $\geqslant$2.5 cm, every branch, live or dead, was cut from the stem and weighed green individually. Each branch was weighed green with any leaves attached, then leaves were clipped from the branch and weighed separately, and the mass of the branch without leaves was determined. A subsample of leaves were weighed green in the field and transported back to the lab for drying. A disk was removed from the mid-section of each branch, to obtain the dry mass to green mass ratio for the branch. Branch disks were measured and weighed and transported back to the lab for drying / processing as described above. All small branches, with a diameter <2.5 cm, were weighed together and a subsample was taken to the lab for drying.

Dry masses were computed for all tree parts using green mass-dry mass ratios computed from sample disks removed from each part which were multiplied by their known green masses; all green parts of all trees were weighed to three significant figures of accuracy. Where multiple disks were available (e.g., from each end of a section), green mass-dry mass ratios were estimated as the weighted average of them, weighted by the cross-sectional area of the disk. All leaves were oven-dried at 70 °C, and woody parts at 105 °C, until reaching 0% moisture content determined by reweighing until dry mass was constant. The green mass used to compute M_1 was the sum of all sections up to 1.3 m. M_2 and M_3 were computed from the sum of the green masses of all main stem sections above 1.3 m and below and above H_C, respectively, with the mass of the shared section where H_C occurred split between them, depending on the location of H_C within that section. The green mass used to compute M_4 was the combined green mass of all the branches, minus the leaves. Green disk volume and oven dry mass of the disk removed at 1.3 m above ground were used to compute basic wood density at breast height, denoted as ρ, following procedures suggested by Williamson and Wiemann (2010). Because all of these trees were deciduous, and some were felled during winter, during different years of the study, leaf data were not available for all the trees. So, leaf biomass was not included in this analysis. Thus, M_W here is the oven dry mass of all tree wood and bark 15 cm above ground level, the sum of $M_1 + M_2 + M_3 + M_4$.

3.2. Data analysis

All analyses were accomplished using functions and packages in the R statistical environment (R Development Core Team, 2010). Eqs. (1) and (2) were fit to the data using ordinary least squares linear regression (OLS) on log-transformed variables. Log transformation was used following standard procedures for testing non-linear allometric equations, to normalize for heteroscedastic variance of mass observed over the large size range of the trees (Goodman et al., 2014). Hayes et al. (1995) demonstrated that fitting the log-transformed allometric function produced more efficient estimates than non-linear least squares estimation. Eq. (2) was fit to the data using general linear modeling, both with and without an intercept. Only models with non-zero coefficients and p-values significant at $\alpha = 0.05$ were accepted.

Eqs. (4) and (5) were fit as a system of equations: $M_W = M_1 + M_2 + M_3 + M_4$, using seemingly unrelated regression

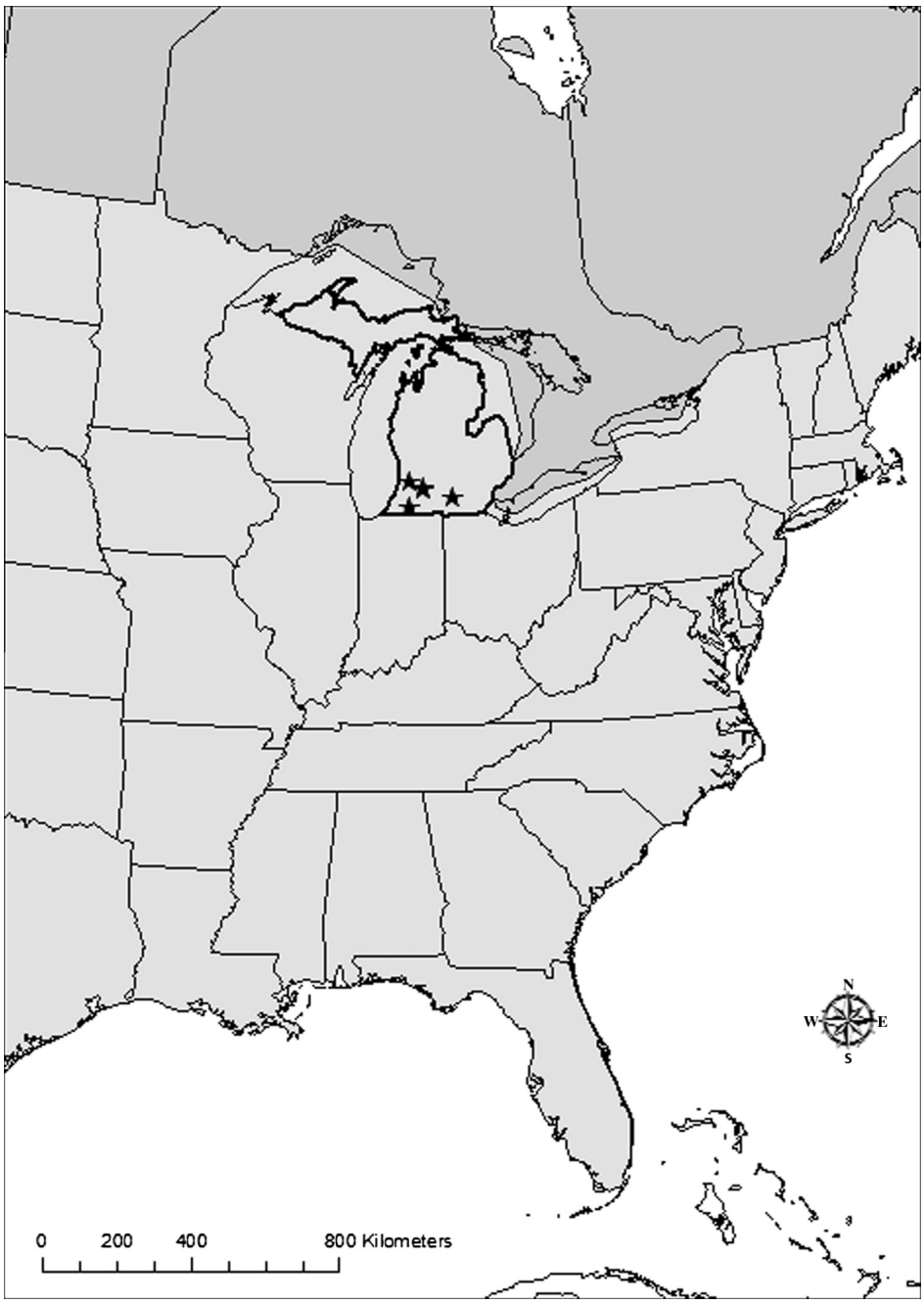

Fig. 2. Map of southeastern North America with locations of forest stands and trees (star symbols). Dark gray-shaded areas are Canada, lighter gray are USA, with the state of Michigan bold-outlined.

(SUR, Parresol, 2001). This preserved correlation among residuals from each component equation in the system. SUR is expected to produce more efficient estimates by weighting the covariance of the residuals from the individual regressions (Parresol, 2001). Eq. (4) was fit as a system of linear equations. Eq. (5) was fit as a system of linear equations, with log-transformed mass components and predictors, for reasons mentioned above. For Eqs. (2a) and (5), scaling was considered proportional if $B_i = 1$ was included in the 95% confidence interval (CI) of model coefficients. Eqs. (4) and (5) were fit using the systemfit package in R (Henningsen and Hamann, 2007). Eq. (6) was fit for each of the four mass components, M_1 through M_4, after log transformation, and summed to obtain predictions of whole tree mass after back-transformation. Fitting the models individually with regression gives the same estimates as SUR for Eq. (6), because the predictor variable (D) is identical for each system component (Parresol, 1999).

Since the coefficient of determination (R^2) of the log-transformed models describes the percentage of variation in the regression associated with log mass; this is denoted hereafter as R^2 log. A second R^2 was computed from the mean squared error of biomass predictions and the variance of measure biomass in the original mass units:

$$R^2 = \frac{\sum_i^n (M_i - \hat{M}_i)^2}{\sum_i^n (M_i - \bar{M}_i)^2} \quad (7)$$

Table 1
Summary statistics for destructively-sampled hardwood tree species sampled from different forest stands in Michigan.

	A. rubrum	*L. tulipifera*	*Q. alba*	*Q. rubra*	*T. americana*	All
# trees	23	14	13	6	8	64
# stands	7	1	4	2	4	17
mean D (cm)	14.9	16.0	14.0	8.7	16.8	14.6
min D (cm)	2.0	1.8	2.5	1.9	5.5	1.8
max D (cm)	30.3	29.4	27.2	17.4	26.4	30.3
mean H (m)	80.6	88.6	72.1	66.7	78.6	79.2
min H (m)	27.5	21.0	27.7	28.0	40.3	21.0
max H (m)	99.7	122.5	109.4	90.1	100.2	122.5
mean W (m)	32.9	33.5	30.8	19.8	29.1	30.9
min W (m)	13.4	13.4	8.7	5.7	12.4	5.7
max W (m)	64.5	64.8	60.4	33.3	44.2	64.8
mean ρ (kg m^{-3})	508	371	608	616	344	486
min ρ (kg m^{-3})	416	269	545	559	295	269
max ρ (kg m^{-3})	650	435	679	724	371	724

D is stem DBH; H is tree total height; W is average crown width; ρ is wood density at 1.3 m.
Study species are *Acer rubrum*, *Liriodendron tulipifera*, *Quercus alba*, *Quercus rubra* and *Tilia americana*.

where M_i and $\hat{M}_i$ are the measured and predicted mass (kg), respectively, for a tree mass component and $\bar{M}_i$ is the mean measured mass of it.

Eq. (7) was used to evaluate the fit of any model with log transformed variables in the original units. Since log-transformation creates a bias in the intercept when predicting biomass, a correction factor (cf) = exp(MSE/2) was applied to back-transformed predictions (Hayes et al., 1995), before applying Eq. (7). Since the correlation coefficient (R^2) can sometimes be a poor estimator of model performance and because the mean squared error (MSE) was in different units for models with log-transformed vs. non-transformed response variables, the Mean Absolute Prediction Error (MAPE, Sileshi, 2014) was used as the primary metric to evaluate the performance of models in comparison to each other:

$$\text{MAPE} = \frac{1}{n}\sum_{i}^{n}\frac{|M_i - \hat{M}_i|}{M_i} \quad (8)$$

Any two models (e.g., A & B) were compared by the % increase or decrease in MAPE (e.g., $[\text{MAPE}_B - \text{MAPE}_A]/[\text{MAPE}_B]$), resulting from switching from one model to the other.

Finally, regression lines fitted to observed versus model-predicted mass values were used to detect model bias (Piñeiro et al., 2008); models with a slope and intercept not significantly different ($\alpha = 0.05$) from one and zero, respectively, were considered to have unbiased prediction.

4. Results

4.1. Tree mass component prediction with variable- vs. fixed- form and density models

The coefficient of proportionality (B) was a statistically significant predictor of hardwood tree mass components in Eqs. (5a)–(5d) (Table 2). Nonetheless, the variable-form, variable-density mass component models, with and without a scaling exponent for proportionality (B_i) (Eqs. (5a)–(5d) and (4a)–(4d), respectively), gave similar predictions of mass components. The R^2 value was nearly identical for each model for each component, but the MAPE showed some differentiation (e.g., (4a) vs. (5a), Table 2). Adding the coefficient B_i to the models decreased the MAPE for components M_1 and M_4, by 4% and 15%, respectively, but increased it for components M_2 and M_3, by 1% and 10%, respectively. Graphical analyses of observed versus predicted values show highly accurate estimation of each biomass component (as indicated slope, intercept and 95% CI of the regression lines), with both versions of the variable-form, variable-density mass component models (compare Eqs. (4a)–(4d) in Fig. 3 and Eqs. (5a)–(5d) in Fig. 4). This indicates that scaling of individual components may be more or less size-dependent, but the net result is that scaling at the whole-tree level is size-dependent.

Both forms of the variable-form, variable-density mass component models (Eqs. (5a)–(5d) and (4a)–(4d), respectively) gave superior predictions of all components of tree mass, when compared to the fixed-form, fixed-density mass component model (Eq. (6)) (Table 2). The MSE of log mass was cut roughly in half for all components when using Eqs. (5a)–(5d) as compared to Eqs. (6a)–(6d), with corresponding reductions in the MAPE of 44%, 57%, 8%, and 40% for components M_1, M_2, M_3, and M_4 respectively. Biomass components predicted only with DBH showed a much lower precision of prediction and greater heteroscedasticity of prediction error, especially for more massive tree components, when compared to the variable-form, variable-density component models (compare Fig. 5 to Figs. 3 and 4). Predicting the mass of the dominant stem in the crown from DBH resulted in a significantly biased (overestimate) of the mass of this component of the tree (Fig. 5).

The R^2 log gave a more liberal impression of the quality of all the models than R^2 expressed in the original units and muted the differences between the different models (e.g., M_2, Table 2). This indicates that a high degree of caution should be used when evaluating models based on R^2 log.

4.2. Allometric scaling of tree components

Examination of the coefficients of the mass component models revealed clear size-dependent (non-isometric) allometry within hardwood trees. From base to branches the power coefficients in Eq. (6) increased: $\beta_1 \approx 1.98$, $\beta_2 \approx 2.35$, $\beta_3 \approx 2.59$, $\beta_4 \approx 2.72$, with statistically different β for the base, trunk and branch components ($\alpha = 0.05$). If allometric relationships were isometric, all parts of the tree should scale to the same power. Coefficients B_1, B_2, and B_4, in Eq. (5), were all statistically different from one, indicating non-proportional scaling of form for M_1, M_2, and M_4. B_1 and B_2 were both significantly less than one, suggesting increased flaring at the bases (M_1) and greater tapering of the trunks (M_2) of trees as they increased in size. B_4 was significantly greater than one, indicting that the branches of hardwoods (M_4) were becoming relatively more massive as the tree increased in size and spread horizontally. This expansion of the crown relative to the truck with increasing size is further supported by the fact that the allometric scaling coefficient β_4, in Eq. (6d), was significantly higher than β_1 and β_2 values for the other components (Table 2). Coefficient B_3, in Eq. (5), was not statistically lower than one, likely due to more highly variable mass-form relationships for the dominant stem in the crown (M_3) (see Fig. 4). These results give further evidence that the scaling of the parts is different than the scaling of the whole tree and that scaling relationships change as the trees increase in size.

4.3. Total mass, main stem and crown mass estimation

The best model for estimating total above-ground woody tree mass (M_W) of hardwood trees was Eq. (2a), when compared to other models in terms of MAPE (Table 3). Eq. (2) was a close second, with only a 4% increase in the MAPE, when omitting the coefficient of proportionality (B, Table 3). Predicting total mass from Eq. (4) resulted in a 14% increase in MAPE over the best model (Eq. (2a)) and predicting total mass from Eq. (5) resulted in a 24%

Table 2
Coefficients and fit statistics for models estimating major components of tree above-ground woody biomass.

Model	Eq. #	Intercept (se)	Slope (se)	MSE	c = exp(MSE/2)	R^2 log	R^2	MAPE
$M_1 = F_1(\rho(\pi/4)D^2H_B)$	[Eq. (4a)]	NA	$9.78 * 10^{-5}$ ($1.30 * 10^{-6}$)	172	–	–	0.975	0.123
$\log(M_1) = \log(F) + B_1 \log(\rho(\pi/4)D^2H_B)$	[Eq. (5a)]	−8.797 (0.198)	0.969 (0.015)†	0.031	1.016	0.984	0.975	0.118
$\log(M_1) = \log(\alpha) + \beta_1 \log(D)$	[Eq. (6a)]	−2.853 (0.150)	1.967 (0.043)^{a}	0.061	1.031	0.971	0.939	0.210
$M_2 = F_2(\rho(\pi/4)D^2(H_C - H_B))$	[Eq. (4b)]	NA	$8.18 * 10^{-5}$ ($1.07 * 10^{-6}$)	5,792	–	–	0.978	0.210
$\log(M_2) = \log(F_2) + B_2 \log(\rho(\pi/4)D^2(H_C - H_B))$	[Eq. (5b)]	−8.030 (0.248)	0.913 (0.017)†	0.075	1.038	0.975	0.977	0.213
$\log(M_2) = \log(\alpha) + \beta_2 \log(D)$	[Eq. (6b)]	−2.806 (0.299)	2.35 (0.086)^{b}	0.242	1.128	0.922	0.800	0.495
$M_3 = F_3(\rho(\pi/4)D^2(H - H_C))$	[Eq. (4c)]	NA	$1.95 * 10^{-5}$ ($7.17 * 10^{-7}$)	13,301	–	–	0.842	0.401
$\log(M_3) = \log(F) + B_3 \log(\rho(\pi/4)D^2(H - H_C))$	[Eq. (5c)]	−10.282 (0.433)	0.962 (0.027)	0.208	1.110	0.946	0.845	0.441
$\log(M_3) = \log(\alpha_3) + \beta_3 \log(D)$	[Eq. (6c)]	−4.320 (0.388)	2.590 (0.115)^{b,c}	0.406	1.225	0.896	0.764	0.481
$M_4 = F_4(\rho(\pi/4)D^2W)$	[Eq. (4d)]	NA	$4.74 * 10^{-5}$ ($1.51 * 10^{-6}$)	28,923	–	–	0.904	0.431
$\log(M_4) = \log(F_4) + B_4 \log(\rho(\pi/4)D^2W))$	[Eq. (5d)]	−10.997 (0.409)	1.059 (0.027)†	0.168	1.088	0.959	0.902	0.365
$\log(M_4) = \log(\alpha_4) + \beta_4 \log(D)$	[Eq. (6d)]	−4.531 (0.353)	2.722 (0.101)^{c,d}	0.335	1.182	0.920	0.717	0.611

ρ is wood density at 1.3 m; D is stem DBH; H is tree total height; H_B is 1.3 m; H_B is the height to the crown base; W is average crown width.
MSE (mean squared error) is used to derive an adjustment (c) to the intercept coefficient (exp(MSE/2) after back-transformation of log-transformed response variables. R^2 log is the coefficient of determination and R^2 is the R^2 coefficient of determination in the original units. MAPE is the mean absolute prediction error.
† Indicates coefficient statistically different from 1 ($\alpha = 0.05$). β values with the same superscripted letter (a–d) are not statistically different.

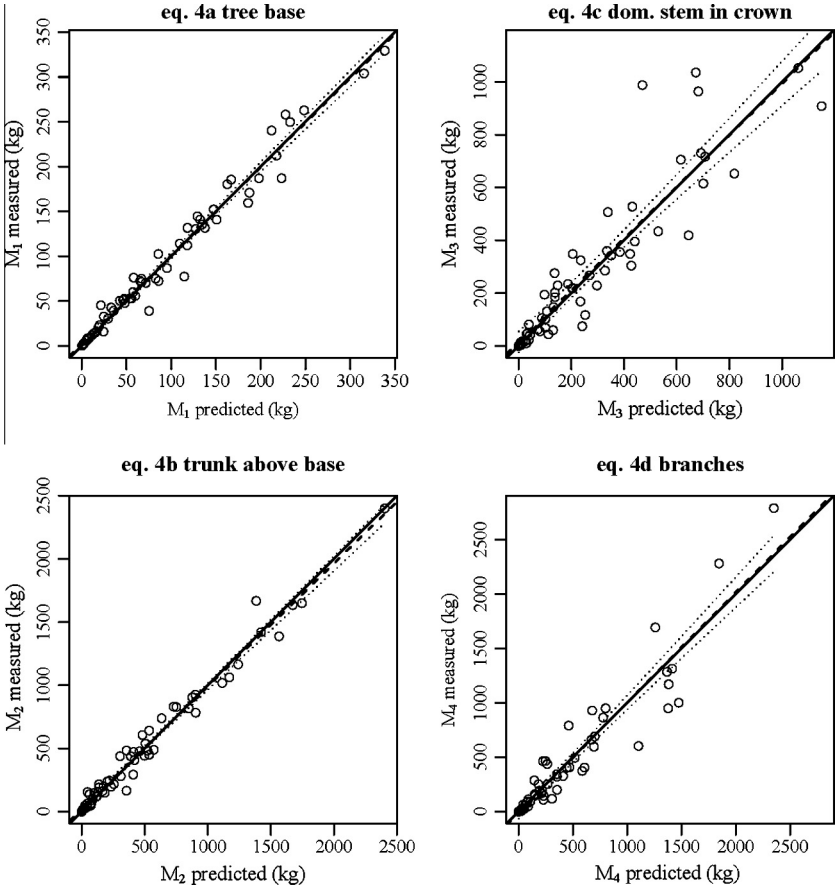

Fig. 3. Measured vs. predicted components of tree mass derived from the variable-form, variable-density component biomass model with a proportionality constant fixed at one (Eq. (4)).

increase in the MAPE over the best model (Table 3), indicating a possible reduction in bias when using Eq. (4) vs. (5) for total mass estimation. However, plots of observed versus predicted values show very little substantive difference total mass estimation between Eqs. (4) and (5) (Fig. 6). The standard allometric equation (Eq. (1)) had an MAPE 63% higher than the best model and the equation predicting total mass from the sum of simple allometric component models (Eq. (6)) had an MAPE 68% higher than the best model.

Predictions of two major components of total mass, main stem mass and crown mass, were also examined graphically side by side (Fig. 6) to better understand total mass estimation from components. Adding mass components $M_1 + M_2 + M_3$ gives the total mass of the main stem and adding components $M_3 + M_4$ gives the total mass of the crown. Plotting observed versus predicted values, both Eqs. (4) and (5) give accurate estimates of total, main stem and crown mass, while Eq. (6) gives biased estimates of all three (as indicated by the slope and 95% CIs of the regression lines, Fig. 6).

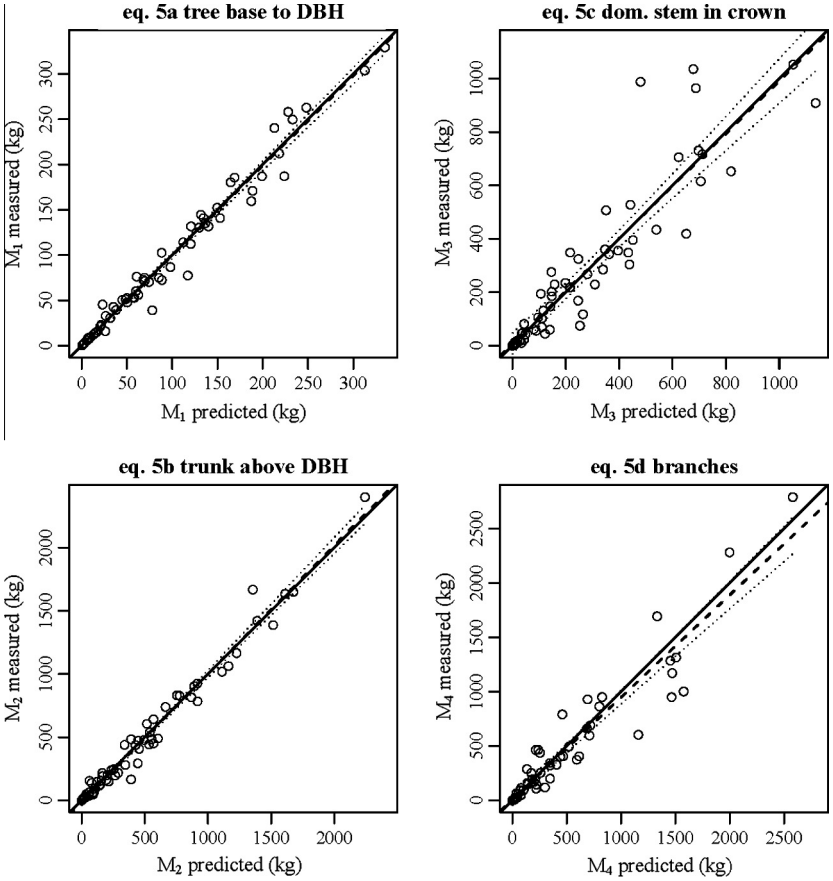

Fig. 4. Measured vs. predicted components of tree mass derived from the variable-form, variable-density component biomass model with a coefficient for proportionality (Eq. (5)).

The superiority of Eqs. (4) and (5) to Eq. (6) in both component and total mass estimation comes in part from knowing the breast-height density of each tree. Two alternative sources for estimating ρ for each tree were also examined to help better understand model performance without this knowledge. Under one scenario, each tree was assigned a species-average breast height wood density, ρ_s, which was computed from the known breast height densities of each tree from each species. This is analogous to sampling some trees of each species, but not knowing the mass of each individual. Under another scenario, a species-specific wood density was taken from published values in the literature (ρ_L) from the USDA Forest Products Laboratory (2010). Inputting these alternative values for ρ into Eq. (5) resulted in an increase in the MAPE 10% and 11%, respectively, for ρ_L and ρ_s, when using them instead of ρ (Table 3). However, the MSE values for Eq. (5) with ρ_L and ρ_s were still half of the MSE for Eq. (6) (Table 3). This demonstrates that the additional dimensional measurements describing within-tree variation in form add important information for obtaining unbiased estimates of tree mass components, distinctive from improved information on tree density.

4.4. Species-specific versus mixed-species models

The variable-form, variable-density component biomass models, with proportionality coefficients (Eqs. (5a)–(5d)), were also fit to each species individually (Table 4). The results suggest that the species-specific models were superior to the mixed-species model, in most cases, for most components, when compared using the MAPE (exceptions are highlighted in bold in Table 4). The most notable exception was a 25% increase in the MAPE relative to the mixed-species model, when Eq. (5) was fit only to *T. americana*. Looking at the coefficients of the species-specific models reveals the divergence of each species from the mixed hardwood species model (compare Tables 2 and 4). The largest differences between the mixed- and species-specific equations were for models of the trunk and branches (Table 4). In terms of the proportionality coefficients, the species-specific models were less likely to show statistically significant differences in size scaling (B_i not statistically different from one, Table 4). However, the sample sizes were reduced when fitting each component model for each species, decreasing the power of the significance test. None of the B_i values estimated for the species-specific models were statistically different from the all-species trend (compare Tables 2 and 4), indicating that species-specific trends were varying around an overall trend of size-dependent allometry for hardwoods.

5. Discussion

5.1. Variable, size-dependent scaling of tree components

The results strongly support the assertion of Niklas (1995) that allometric scaling relationships for trees are size-dependent. Form relationships of major hardwood components were shown to change with increasing size, even over the limited geographic range (100's of km, Fig. 2) and range of species examined here. The clear difference in the scaling of different tree parts with DBH (Eqs. (6a)–(6d)) is more evidence that isometric growth is more likely a special case, rather than the norm in tree allometry (Stevens, 2009). Such variable, size-dependent allometry highlights limitations to the common approach of estimating tree mass

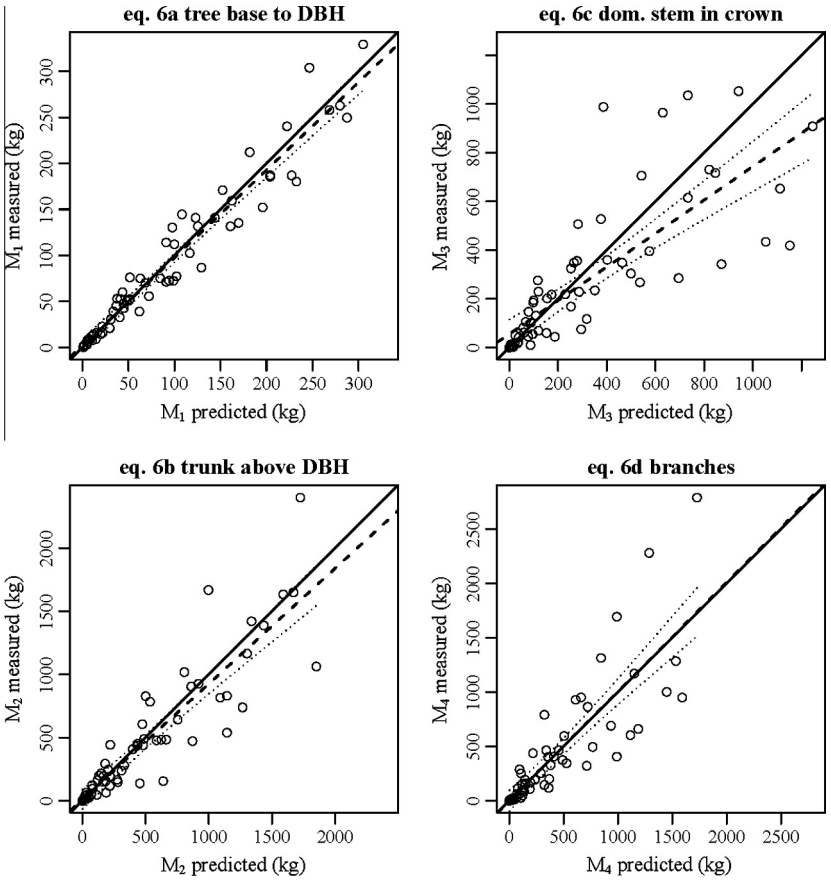

Fig. 5. Measured vs. predicted components of tree mass derived from the fixed-form, fixed-density component biomass model (Eq. (6)).

Table 3
Coefficients and fit statistics for models for estimating total above-ground woody biomass.

Model	Eq. #	Intercept (se)	Slope (se)	MSE	c = exp(MSE/2)	R^2 log	R^2	MAPE
$\log(M_W) = \log(\alpha) + \beta \log(D)$	[Eq. (1)]	−2.104 (0.167)	2.431 (0.048)	0.075	1.038	0.976	0.906	0.233
$M_W = F(\rho(\pi/4)D_2H)$	[Eq. (2)]	NA	$6.30 * 10^{-5}$ ($8.88 * 10^{-7}$)	39,880	–	–	0.987	0.149
$\log(M_W) = \log(F) + B\log(\rho(\pi/4)D^2H)$	[Eq. (2a)]	−9.070 (0.198)	0.962 (0.012)†	0.033	1.016	0.989	0.967	0.143
$M_W = M_1 + M_2 + M_3 + M_4$	[Eq. (4)]	–	–	45,218	–	–	0.972	0.163
$M_W = M_1 + M_2 + M_3 + M_4$	[Eq. (5)]	–	–	43,281	–	–	0.974	0.177
$M_W = M_1 + M_2 + M_3 + M_4$	[Eq. (5)] w ρ_s	–	–	74,640	–	–	0.955	0.193
$M_W = M_1 + M_2 + M_3 + M_4$	[Eq. (5)] w ρ_L	–	–	73,784	–	–	0.955	0.191
$M_W = M_1 + M_2 + M_3 + M_4$	[Eq. (6)]	–	–	173,824	–	–	0.894	0.240

D is stem DBH; H is tree total height; H_B is 1.3 m; H_B is the height to the crown base; W is average crown width; ρ is wood density at 1.3 m; ρ_s is wood density at 1.3 m from a sample of trees; ρ_s is wood density at 1.3 m from published literature.
MSE (mean squared error) is used to derive an adjustment (c) to the intercept coefficient (exp(MSE/2) after back-transformation of log-transformed response variables.
R^2 log is the coefficient of determination and R^2 is the R^2 coefficient of determination in the original units.
MAPE is the mean absolute prediction error.
† Indicates coefficient significantly different from 1 ($\alpha = 0.05$).

components from DBH and also why summing such estimates created a bias in total mass estimation that increased as trees increased in DBH (Fig. 6). This suggests that incorporating size-dependence may be particularly important for extrapolating allometric models to predict component mass for larger trees, which often contain the bulk of the biomass found in forests.

By describing within-tree differences in tree form, in a statistical modeling framework that considers size-dependent allometry, the variable-form, variable-density mass component model allowed for accurate prediction of tree mass components and total tree mass, across a range of tree sizes and forest conditions for major hardwood species in Michigan. It is useful to speculate how the results might have changed if applied to a different set of trees and stands. Recent studies have shown that hardwoods differ significantly from conifers in terms of their allometric scaling (e.g., "evergreenness" effects height-diameter relationships, Ducey, 2012). One might expect hardwoods to show a higher variability in scaling of the crown and trunk, relative to conifers, because hardwoods tend to show weaker epinastic control, allowing for greater relative shifts to expansion of branches in the crown relative to allocation to the main stem (Oliver and Larson, 1996). One might also expect to find less variation in tree form if the trees were taken from only one stand or from plantations, rather than multiple, natural stands, as was done here, due to the homogenizing effects of stand conditions and management. A recent study by Valentine et al. (2012) showed that even under the homogenizing conditions of coniferous

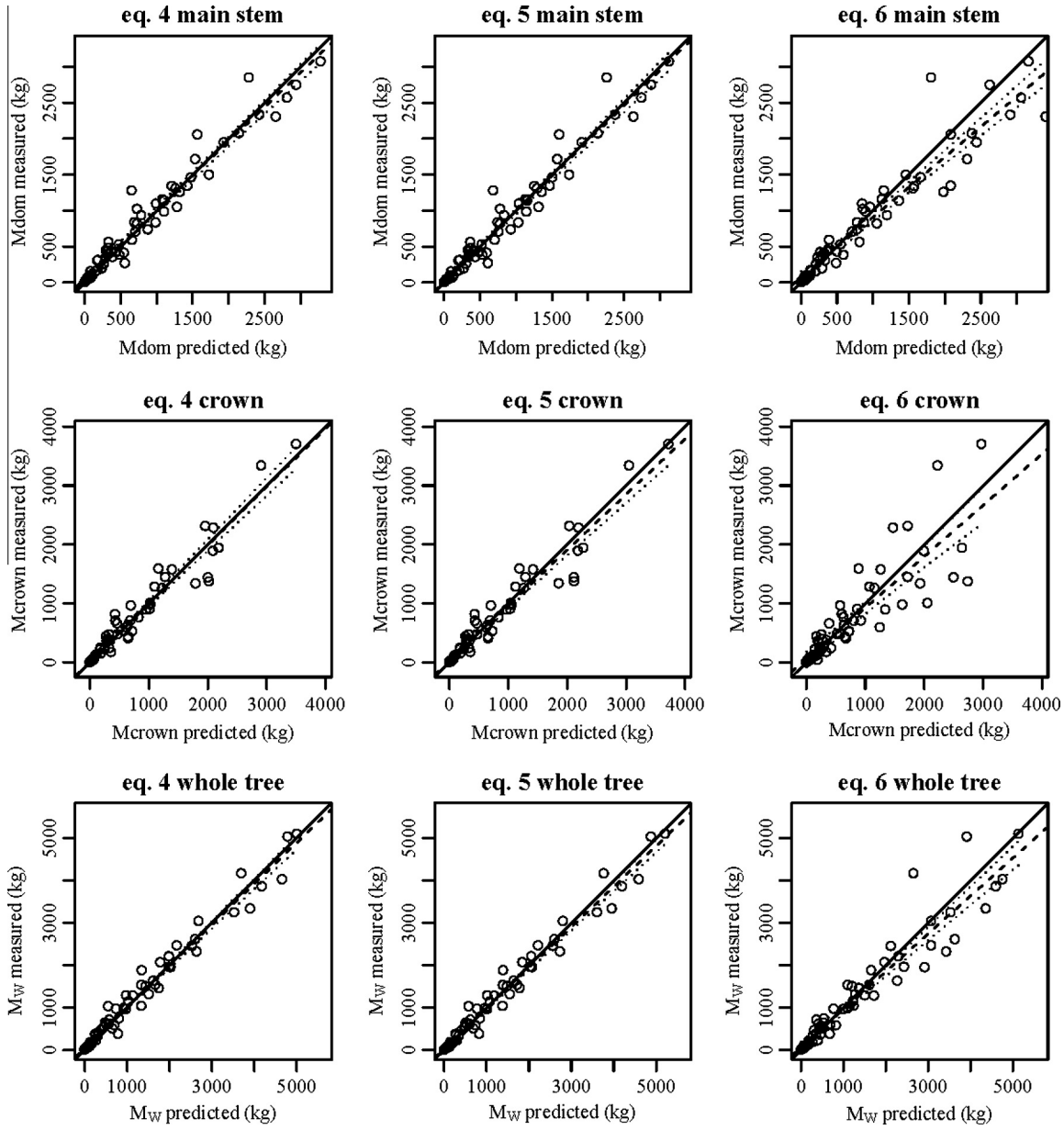

Fig. 6. Measured vs. predicted main stem, crown and whole-tree mass from three different additive models (Eqs. (4)–(6)).

plantations, in the isolated situation of a closed stand with approximately constant crown length, the assumption of isometric relationships between crown and stem characteristics were not quite met (though the variable-form model was only slightly superior). However, Bravo-Oviedo et al. (2014) noted that even the special case identified by Valentine et al. (2012) should be considered as "one possible value within a [scaling] ratio that changes over time as a function of ontogeny, stand history and climatic conditions". Hence, models which incorporate variable allometry should be the standard for robust estimation of tree form and biomass.

5.2. Intra- vs. inter-specific variation in scaling relationships

Allometric scaling relationships are evolutionarily constrained to assure that tree species can survive and reproduce in different environments. For example, the mechanical stability of trees is limited by the relative size and configuration of branches in their crowns (James et al., 2006). For tree biomass equations, such evolutionary constraints are typically implicit in species-specific coefficients. One goal of this study was to see how robust the new models could be across multiple species drawn from different stands. Species-specific models were found superior to the mixed species models, in most cases examined. However, the results demonstrated that a generalized mixed-species model (Eq. (5)) can fit as well as, or even better than, a species-specific model, in certain cases, and that intraspecific variation in form coefficients can be high, such that species-specific differences might not be statistically differentiable over varying forest conditions (Table 4). One possible explanation, for cases where the mixed-species models gave better predictions, is that a few trees with anomalous forms were dominating the model, whereas the mixed-species model drew from a much wider range of tree forms and better captured morphological variability in hardwood growth form in the model coefficients. In support of the latter, the worst species-specific models in this study were those with lower numbers of sample trees relative to the number of stands they were drawn from (*Quercus alba*, *Quercus rubra* and *Tilia americana*, Tables 1 and 4). Together, these results support the idea that trees

Table 4
Coefficients and fit statistics for species-specific models for Eqs. (5a)–(5d).

Model		Intercept (se)	Slope (se)	MSE	c = exp(MSE/2)	R^2 log	R^2	MAPE	MAPE · mixed
$\log(M_1) = \log(F) + B_1\log(\rho(\pi/4)D^2H_B)$	[Eq. (5a)]								
A. rubrum		-8.616 (0.193)	0.957 (0.014)†	0.009	1.009	0.995	0.975	0.078	0.079
L. tulipifera		-9.233 (0.235)	1.002 (0.018)	0.014	1.014	0.995	0.989	0.098	0.099
Q. alba		-8.693 (0.620)	0.954 (0.047)	0.058	1.060	0.971	0.974	0.164	0.180
Q. rubra		-8.306 (0.738)	0.925 (0.060)	0.052	1.053	0.978	0.815	0.138	0.157
T. americana		-7.858 (1.050)	0.911 (0.079)	0.057	1.059	0.948	0.976	0.131	0.142
$\log(M_2) = \log(F_2) + B_2\ \log(\rho(\pi/4)D^2(H_C - H_B))$	[Eq. (5b)]								
A. rubrum		-7.976 (0.912)	0.912 (0.020)†	0.028	1.028	0.988	0.983	0.128	0.376
L. tulipifera		-7.601 (0.273)	0.891 (0.019)†	0.034	1.035	0.993	0.993	0.129	0.154
Q. alba		-8.276 (0.868)	0.921 (0.058)	0.189	1.208	0.927	0.934	0.298	0.394
Q. rubra		-9.813 (0.308)	1.023 (0.022)	0.014	1.014	0.997	0.976	0.089	0.376
T. americana		-7.308 (0.689)	0.871 (0.046)†	0.073	1.076	0.966	0.989	0.183	**0.156**
$\log(M_3) = \log(F) + B_3\log(\rho(\pi/4)D^2(\mathrm{H}\text{-}H_C))$	[Eq. (5c)]								
A. rubrum		-10.253 (0.590)	0.967 (0.037)	0.090	1.094	0.967	0.874	0.251	**0.241**
L. tulipifera		-9.265 (0.830)	0.907 (0.053)†	0.203	1.225	0.952	0.813	0.397	**0.380**
Q. alba		-10.841 (0.894)	0.987 (0.058)	0.260	1.297	0.948	0.758	0.465	0.618
Q. rubra		-10.006 (1.675)	0.913 (0.118)	0.390	1.477	0.389	0.415	0.555	0.960
T. americana		-11.084 (1.524)	1.014 (0.098)	0.251	1.285	0.902	0.836	0.422	0.452
$\log(M_4) = \log(F_4) + B_4\log(\rho(\pi/4)D^2\mathrm{W}))$	[Eq. (5d)]								
A. rubrum		-10.742 (0.674)	1.046 (0.044)	0.129	1.138	0.961	0.896	0.310	**0.306**
L. tulipifera		-10.322 (0.594)	1.002 (0.044)	0.087	1.091	0.982	0.951	0.259	0.405
Q. alba		-12.364 (0.893)	1.145 (0.059)†	0.178	1.195	0.948	0.948	0.363	0.456
Q. rubra		-11.193 (2.146)	1.081 (0.157)	0.545	1.725	0.891	0.531	0.072	0.543
T. americana		-10.607 (1.442)	1.050 (0.096)	0.149	1.161	0.938	0.728	0.309	**0.185**
$M_W = M_1 + M_2 + M_3 + M_4$	[Eq. (5)]								
A. rubrum		–	–	46,092	–	0.990	0.970	0.115	0.117
L. tulipifera		–	–	14,471	–	0.994	0.992	0.109	0.138
Q. alba		–	–	57,202	–	0.954	0.977	0.218	0.290
Q. rubra		–	–	11,029	–	0.999	0.951	0.144	0.259
T. americana		–	–	45,028	–	0.969	0.937	0.229	**0.183**

D is stem DBH; H is tree total height; H_B is 1.3 m; H_B is the height to the crown base; W is average crown width; ρ is wood density at 1.3 m; ρ_s is wood density at 1.3 m from a sample of trees; ρ_s is wood density at 1.3 m from published literature.
MSE (mean squared error) is used to derive an adjustment (c) to the intercept coefficient (exp(MSE/2) after back-transformation of log-transformed response variables.
R^2 log is the coefficient of determination and R^2 is the R^2 coefficient of determination in the original units.
MAPE is the mean absolute prediction error for the model listed and MAPE · mixed is the prediction for the species from the mixed-species model. Bold values for MAPE · mixed < MAPE.
Species are *Acer rubrum*, *Liriodendron tulipifera*, *Quercus alba*, *Quercus rubra* and *Tilia americana*.
† Indicates coefficient significantly different from 1 ($\alpha = 0.05$).

show a high degree of intraspecific plasticity in allocation of biomass to different parts, despite a significant underlying genetic model controlling the branching architecture that defines tree form (Barthélémy and Caraglio, 2007; Dardick et al., 2013).

Given the apparently high degree of inter- and intra-specific variation in tree allometry and typical data limitations, tree biomass equations might be better designed to be robust to accommodate a wide range of tree forms. Species-specific models are likely to be based on relatively small data sets (Sileshi, 2014) and over a limited range of diameters, relative to the population to which they will be applied (Weiskittel et al., 2015). This is because collecting data to calibrate biomass equations is expensive and time-consuming, as it requires felling a tree, dividing it into various components (e.g. branches, trunk, etc. . .) and accurately weighing the material in the field. Data is particularly limited for rare or even uncommon tree species and for very large trees (Goodman et al., 2014). With generally low sampling intensities for calibration data and high variability in tree populations being the norm for development and application of tree biomass estimations, respectively (Weiskittel et al., 2015), there is potential for a generalized modeling approach that draws from the strength of all available data, from all trees, of all species and growth forms, even to estimate mass for a specific population of trees.

5.3. Economic and ecological relevance of better component mass estimates

The generalized, variable-form, variable-density tree component mass model, introduced here, expands the form factor model (Eq. (2) or (2a)), which had been previously demonstrated to provide generalized prediction of whole-tree mass across a wide range of species and forest conditions (e.g., Cannell, 1984; Chave et al., 2005), and now allows for accurate estimation of the mass of ecologically and economically relevant tree components. This generality of the model could help improve biomass inventories, such as the US national forest inventory, especially over large spatial domains, or wherever there are large numbers of co-occurring species (e.g., the tropics, Chave et al., 2014) and/or widely varying silvicultural conditions.

Improving biomass component estimation, with explicit linkages to the merchantability of those components, has been an explicit goal of FIA efforts to produce better national tree biomass equations for the USA (Domke et al., 2012). The currently-available Jenkins et al. (2003) equations predict biomass component fractions with extremely low accuracy and total mass based on fixed component-DBH relationships. Also, the Jenkins et al., biomass equations do not provide a clear way to connect biomass components to the merchantable components of mass. This deficiency led to development of the "component ratio method" (CRM, Woodall et al., 2011), which converts merchantable bole volume into bole mass and then computes remaining biomass components as fractions of a total, derived from Jenkins et al.,'s (2003) total mass- and component-DBH relationships. While the CRM provides a direct way to connect tree merchantable volume estimates with total mass and biomass components (Domke et al., 2012), it does so using component ratios derived from two incompatible models of the same tree. The approach of Jenkins et al. (2003) highlights

the difficulty of predicting the relative size of parts from a whole-tree estimate, without the addition of any new information beyond DBH. The CRM highlights the difficulty of predicting a whole tree from a disembodied part, in that case, the merchantable bole, whose dimensionality is based on an economic value judgement, rather than a biologically relevant dimension of the tree. Both of these approaches are based on purely empirical relationships, rather than biological principles, which likely limits their robustness. The new model framework presented here, by contrast, explicitly incorporates the variability of whole-tree allometry, as a biological phenomenon influencing tree utilization, and expresses the tree as the sum of interrelated parts. As trees are increasingly forced to adapt to novel climates, tree biomass models that offer biologically meaningful coefficients to index tree form should be of increasing value for decision-makers (Weiskittel et al., 2015).

Better prediction of mass components did provide less accurate estimates of whole-tree mass relative to a 'best' model that *only* predicts total mass. However, this is a very strict test of the performance of a model designed to predict components, as it is typical only to compare different methods for constructing additive models to each other (e.g., Parresol, 1999; Bi et al., 2004). If total mass is the *only* concern, these results suggest that a total mass model (like Eq. (2a)) may be preferable to one that builds total mass from its components. However, interest in economically and biologically relevant biomass inventories has been steadily growing for decades (Parresol, 1999). For example, Zakrzewski and Duchesne recently (2012) suggested a future forest management regime, where carbon stored in harvested wood might be on par, economically, with timber products. Ultimately, it is up to model builders and users to decide how much emphasis to place on the accuracy of total versus component masses. Of course, compatibility between whole-tree and component mass can be assured by forcing additivity of the biomass components (Brandeis et al., 2006), but improvements to mass prediction can be relatively small (Bi et al., 2004) and there are significant problems associated with restricting coefficients during estimation (Parresol, 1999). This research suggests that the biggest gains in component mass estimation are likely to come from more complex models that better characterize the relationships between tree parts.

5.4. Cost-benefit considerations for applying more complex tree mass models

Many studies prior to this have shown that improvements can be made by adding predictors other than DBH to improve tree biomass estimation. The most common is tree height, because height-diameter relationships vary across a range of ecological conditions (Ketterings et al., 2001; Ducey, 2012; Feldpausch et al., 2012; Chave et al., 2014). Measurements of crown dimensions have been recently emphasized as critical to improving tree biomass estimation, including measurements of crown length (Mäkelä and Valentine, 2006), crown spread (Goodman et al., 2014) and the diameter of the largest branch in a tree (MacFarlane, 2011). Thus, it was not surprising that predictions of crown components were less accurate under the fixed-form, fixed-density approach (Eq. (6)). It was surprising, though, how much worse the DBH-only approach was at predicting the trunk and dominant stem components. This supports the theory that tapering of the trunk is strongly affected by accumulated branching events and branch losses over a tree's lifetime (Niklas, 1995; Mäkelä and Valentine, 2006; MacFarlane et al., 2014).

The most common reason not to incorporate additional measurements in forest inventories has been cost, but recent advances in forest inventory technology, including laser range finders, digital optical dendrometers and digital hypsometers have dramatically increased the accuracy of, and time efficiency for, measuring tree heights and crown dimensions. The increasingly widespread use of remote sensing technologies, such as LiDAR, will increasingly allow for improved, lower-cost estimation of the vertical profiles of trees and branching architecture (Côté et al., 2009). Concordantly, tree biomass models that better describe the three-dimensional structure of tree form should better align with attempts to improve forest biomass estimates via remote sensing.

Wood density (specific gravity) has also been shown to be an important predictor in whole-tree mass models prior to this study (Cannell, 1984; Chave et al., 2005), but the necessity to input a wood density value for each tree is a major issue for application. For standing trees, either cores would need to be extracted from a sample of trees to obtain wood density estimates for the population (Wiemann and Williamson, 2011), or, trees would need to be assigned published values (as suggested by Chave et al., 2005). Unlike previous studies, this study explicitly tested the effect of employing these latter strategies and found that they added about 10% to the prediction error (MAPE). Literature values, which are easy to obtain, might be further improved by incorporating knowledge of geographic and phylogenetic constraints on wood density variation (Swenson and Enquist, 2007). Published wood density values for trees are typically breast-height estimates, but some models have incorporated vertical mass variation within the tree to improve biomass prediction, generally for the main stem of the tree (Jordan et al., 2006; Zakrzewski and Duchesne, 2012). Recently Ver Planck and MacFarlane (2015) applied the density-integral approach to estimate both branch and main stem mass from models of within-tree variation in mass and volume and showed that wood density variation within the main stem and the branches of hardwoods was highly complex. So, for practical reasons, using only wood density at breast height and assuming some proportional relationship within trees (e.g., between stems and branches, Swenson and Enquist, 2008) may give the greatest predictive power at the lowest cost.

Acknowledgement

This research was funded by a Joint Venture Agreement between Michigan State University and the USDA Forest Service Forest Inventory and Analysis Program, Northern Region. Part of D.W. MacFarlane's time was supported with funds from Michigan AgBioResearch through the USDA National Institute of Food and Agriculture. The author would like to thank the field crew at W.K. Kellogg Experimental Forest for many hours of tedious data collection and Anthony Russel for writing efficient R code to compile complex tree data.

References

Adu-Bredu, S., Bi, A., Bouillet, J., Mé, M., Kyei, S., Saint-André, L., 2008. An explicit stem profile model for forked and un-forked teak (Tectona grandis) trees in West Africa. Forest Ecol. Manage. 255, 2189–2203.

Henningsen, Arne, Hamann, Jeff D., 2007. Systemfit: a package for estimating systems of simultaneous equations in R. J. Stat. Softw. 23 (4), 1–40, <http://www.jstatsoft.org/v23/i04/>.

Barthélémy, D., Caraglio, Y., 2007. Plant architecture: a dynamic, multilevel and comprehensive approach to plant form, structure and ontogeny. Ann. Bot. 99, 375–407.

Bechtold, W.A., Patterson, P.J., 2005. The enhanced forest inventory and analysis program – national sampling design and estimation procedures. USDA For. Serv. Gen. Tech. Rep. SRS-80, pp. 85.

Bi, H., Turner, J., Lambert, M.J., 2004. Additive biomass equations for native eucalypt forest trees of temperate Australia. Trees 18, 467–479.

Brandeis, T.J., Delaney, M., Parresol, B.R., Royer, L., 2006. Development of equations for predicting Puerto Rican subtropical dry forest biomass and volume. For. Ecol. Manag. 233, 133–142.

Bravo-Oviedo, A., del Río, M., Calama, R., Valentine, H.T., 2014. New approaches to modelling cross-sectional area to height allometry in four Mediterranean pine species. Forestry 87, 399–406.

Cannell, M.G.R., 1984. Woody biomass of forest stands. For. Ecol. Manage. 8, 299–312.

Chave, J., Andalo, C., Brown, S., et al., 2005. Tree allometry and improved estimation of carbon stocks and balance in tropical forests. Oecologia 145, 87–99.

Chave, J., Coomes, D., Jansen, S., Lewis, S.L., Swenson, N.G., Zanne, A.E., 2009. Towards a worldwide wood economics spectrum. Ecol. Lett. 12, 351–366.
Chave, J., Réjou-Méchain, M., Búrquez, A., Chidumayo, E., Colgan, M.S., Delitti, W.B.C., Duque, A., Eid, T., Fearside, P.M., Goodman, R.C., Henry, M., Martínez-Yrízar, A., Mugasha, W.A., Muller-Landau, H.C., Mencuccini, M., Nelson, B.W., Ngomanda, A., Nogueira, A., Ortiz-Malavassi, E., Pélissier, R., Ploton, P., Ryan, C.M., Saldarriaga, J.G., Vieilledent, G., 2014. Improved allometric models to estimate the aboveground biomass of tropical trees. Glob. Change Biol. 20, 3177–3190.
Côté, J.F., Widlowski, J.L., Fournier, R.A., Verstraete, M.M., 2009. The structural and radiative consistency of three-dimensional tree reconstructions from terrestrial lidar. Remote Sens. Environ. 113, 1067–1081.
Dardick, C., Callahan, A., Horn, R., Ruiz, K.B., Zhebentyayeva, T., Hollender, C., Whitaker, M., Abbott, A., Scorza, R., 2013. PpeTAC1 promotes the horizontal growth of branches in peach trees and is a member of a functionally conserved gene family found in diverse plants species. Plant J. 75, 618–630.
Dickmann, D.I., 2004. Michigan Forest Communities. 1-56525, ISBN No-109-2. Michigan State University Extension. 158 pp.
Domke, G.M., Becker, D.R., D'Amato, A.W., Ek, A.R., Woodall, C.W., 2012a. Carbon emissions associated with the procurement and utilization of forest harvest residues for energy, Northern Minnesota, USA. Biomass Bioenergy 36, 141–150.
Domke, G.M., Woodall, C.W., Smith, J.E., Westfall, J.A., McRoberts, R.E., 2012b. Consequences of alternative tree-level biomass estimation procedures on U.S. forest carbon stock estimates. For. Ecol. Manage. 270, 108–116.
Ducey, M.J., 2012. Evergreenness and wood density predict height–diameter scaling in trees of the northeastern United States. For. Ecol. Manage. 279, 21–26.
Egnell, G., Valinger, E., 2003. Survival, growth, and growth allocation of planted Scots pine trees after different levels of biomass removal in clear-felling. For. Ecol. Manage. 177, 65–74.
Eloy, C., 2011. Leonardo's rule, self-similarity, and wind-induced stresses in trees. Phys. Rev. Lett. 107, 258101.
Enquist, B.J., 2002. Universal scaling in tree and vascular plant allometry: toward a general quantitative theory linking plant form and function from cells to ecosystems. Tree Physiol. 22 (15–16), 1045–1064.
FAO, 2010. Global Forest Resources Assessment 2010. FAO Forestry Paper, 163. Food and Agriculture Organization of the United Nations, Rome. 378 p.
Feldpausch, T.R. et al., 2012. Tree height integrated into pantropical forest biomass estimates. Biogeosciences 9, 3381–3403.
Forest Products Laboratory, 2010. Wood Handbook—Wood as an Engineering Material. General Technical Report FPL-GTR-190. U.S. Department of Agriculture, Forest Service, Forest Products Laboratory, Madison.
Goodman, R.C., Phillips, O.L., Baker, T.R., 2014. The importance of crown dimensions to improve tropical tree biomass estimates. Ecol. Appl. 24 (4), 680–698.
Gray, H.R., 1966. Principles of forest tree and crop volume growth: a mensuration monograph. Aust. Bull. For. Timber. Bur. 42.
Hayes, D.B., Brodziak, J.K.T., O'Gorman, J.B., 1995. Efficiency and bias of estimators and sampling designs for determining length–weight relationships of fish. Can. J. Fish. Aquat. Sci. 52, 84–92.
Huxley, J.S., Tessier, G., 1936. Terminology of relative growth. Nature 137, 780–781.
James, K., Haritos, N., Ades, P., 2006. Mechanical stability of trees under dynamic loads. Am. J. Bot. 93, 1522–1530.
Jenkins, J.C., Chojnacky, D.C., Heath, L.S., Birdsey, R.A., 2003. National-scale biomass estimators for United States tree species. Forest Sci. 49, 12–35.
Jordan, L., Souter, R., Parresol, B., Daniels, R.F., 2006. Application of the algebraic difference approach for developing self-referencing specific gravity and biomass equations. For. Sci. 52 (1), 81–92.
Ketterings, Q.M., Coe, R., van Noordwijk, M., Ambagau, Y., Palm, C.A., 2001. Reducing uncertainty in the use of allometric biomass equations for predicting above-ground tree biomass in mixed secondary forests. For. Ecol. Manage. 146, 199–209.
Kozak, A., 2004. My last words on taper equations. Forest. Chron. 80 (4), 507–515.
MacFarlane, D.W., 2010. Predicting branch to bole volume scaling relationships from varying centroids of tree bole volume. Can. J. For. Res. 40 (12), 2278–2289.
MacFarlane, D.W., 2011. Allometric scaling of branch volume in hardwood trees in Michigan, USA: implications for improvements in above-ground forest carbon biomass inventories. For. Sci. 57 (6), 451–459.
MacFarlane, D.W., Kuyah, S., Mulia, R., Dietz, J., Muthuri, C., Van Noordwijk, M., 2014. Evaluating a non-destructive method for calibrating tree biomass equations derived from tree branching architecture. Trees 28, 807–817.
Mäkelä, A., Valentine, H.T., 2006. Crown ratio influences allometric scaling in trees. Ecology 87 (12), 2967–2972.
Muhairwe, C.K., 1994. Tree form and taper variation over time for interior lodgepole pine. Can. J. For. Res. 24, 1904–1913.
Niklas, K.J., 1995. Size-dependent allometry of tree height, diameter and trunk-taper. Ann. Bot. 75, 217–227.
Oliver, C.D., Larson, B.C., 1996. Forest Stand Dynamics, update ed. John Wiley and Sons, Inc., New York, 520 p..
Parresol, B.R., 1999. Assessing tree and stand biomass: a review with examples and critical comparisons. For. Sci. 45 (4), 573–593.
Parresol, B.R., 2001. Additivity of nonlinear biomass equations. Can. J. For. Res. 31, 865–878.
Piñeiro, G., Perelman, S., Guerschman, J.P., Paruelo, J.M., 2008. How to evaluate models: observed vs predicted or predicted vs observed. Ecol. Model. 216, 316–322.
R Development Core Team, 2010. R: A Language and Environment for Statistical Computing. R Foundation for Statistical Computing, Vienna, Austria. <http://www.R-project.org>. ISBN 3-900051-07-0.
Stevens, C.F., 2009. Darwin and Huxley revisited: the origin of allometry. J. Biol. 8 (14), 1–7.
Sileshi, G.W., 2014. A critical review of forest biomass estimation models, common mistakes and corrective measures. For. Ecol. Manage. 329, 237–254.
Swenson, N.G., Enquist, B.J., 2007. Ecological and evolutionary determinants of a key plant functional trait, wood density, and its community-wide variation across latitude and elevation. Am. J. Bot. 94, 451–459.
Swenson, N.G., Enquist, B.J., 2008. The relationship between stem and branch wood specific gravity and the ability of each measure to predict leaf area. Am. J. Botany 95 (4), 516–519.
USEPA, 2014. Forest sections of the Land use change and forestry chapter, and Annex. In: US Environmental Protection Agency, Inventory of US Greenhouse Gas Emissions and Sinks: 1990–2012. EPA 430-R-14-003. <http://www.epa.gov/climatechange/emissions/usinventoryreport.html> (June 2013).
Van Noordwijk, M., Mulia, R., 2002. Functional branch analysis as tool for fractal scaling above- and belowground trees for their additive and non-additive properties. Ecol. Model. 149, 41–51.
Valentine, H.T., Gregoire, T.G., 2001. A switching model of bole taper. Can. J. For. Res. 31 (8), 1400–1409.
Valentine, H.T., Mäkelä, A., Green, E.J., Amateis, R.L., Mäkinen, H., Ducey, M.J., 2012. Models relating stem growth to crown length dynamics: application to loblolly pine and Norway spruce. Trees 26, 469–478.
Ver Planck, N.R., MacFarlane, D.W., 2014. Modelling vertical allocation of tree stem and branch volume for hardwoods. Forestry 00, 1–16. http://dx.doi.org/10.1093/forestry/cpu007.
Ver Planck, N.R., MacFarlane, D.W., 2015. A vertically integrated whole-tree biomass Model. Trees 29, 449–460.
Weiskittel, A.R., MacFarlane, D.W., Radtke, P.J., Affleck, D.L.R., Hailemariam, T., Westfall, J.A., Woodall, C.W., Coulston, J.W., 2015. A call to improve methods for estimating tree biomass for regional and national assessments. J. Forest. 113, http://dx.doi.org/10.5849/jof.14-091.
West, G.B., Brown, J.H., Enquist, B.J., 1999. The fourth dimension of life: fractal geometry and allometric scaling of organisms. Science 284 (5420), 1677–1679.
Wiemann, M.C., Williamson, G.B., 2011. Testing a novel method to approximate wood specific gravity of trees. For. Sci. 58 (6), 577–591.
Williamson, G.B., Wiemann, M.C., 2010. Measuring wood specific gravity... correctly. Am. J. Bot. 97 (3), 519–524.
Woodall, C.W., Heath, L.S., Domke, G.M., Nichols, M.C., 2011. Methods and equations for estimating aboveground volume, biomass, and carbon for trees in the U.S. forest inventory, 2010. Gen. Tech. Rep. NRS-88. U.S. Department of Agriculture, Forest Service, Northern Research Station, Newtown Square, PA, 30 p.
Zakrzewski, W.T., MacFarlane, D.W., 2006. Regional stem profile model for cross border comparisons of harvested red pine (Pinus resinosa Ait.) in Ontario and Michigan. For. Sci. 52 (4), 468–475.
Zakrzewski, W.T., Duchesne, I., 2012. Stem biomass model for jack pine (*Pinus banksiana* Lamb.) in Ontario. For. Ecol. Manage. 279 (112–120), 2012.
Zeide, B., Pfeifer, P., 1991. A method for estimation of fractal dimension of tree crowns. For. Sci. 37 (5), 1253–1265.